

Research Article

Integrated Bioinformatics Analysis of Hub Genes and Pathways in Anaplastic Thyroid Carcinomas

Xueren Gao ¹, Jianguo Wang,¹ and Shulong Zhang²

¹Department of Pediatric Endocrinology/Genetics, Xinhua Hospital, School of Medicine, Shanghai Jiao Tong University, Shanghai 200092, China

²Department of General Surgery, Xuhui District Central Hospital of Shanghai, Shanghai 200031, China

Correspondence should be addressed to Xueren Gao; gaoxueren@xinhuaamed.com.cn

Received 2 August 2018; Revised 23 October 2018; Accepted 5 November 2018; Published 13 January 2019

Academic Editor: Rosaria Meccariello

Copyright © 2019 Xueren Gao et al. This is an open access article distributed under the Creative Commons Attribution License, which permits unrestricted use, distribution, and reproduction in any medium, provided the original work is properly cited.

Anaplastic thyroid carcinoma (ATC) is a very rare malignancy; the pathogenesis of which is still not fully understood. The aim of the present study was to identify hub genes and pathways in ATC by microarray expression profiling. Two independent datasets (GSE27155 and GSE53072) were downloaded from GEO database. The differentially expressed genes (DEGs) between ATC tissues and normal thyroid tissues were screened out by the limma package and then enriched by gene ontology (GO) and KEGG pathway analysis. The hub genes were selected by protein-protein interaction (PPI) analysis. A total of 141 common upregulated and 87 common downregulated genes were screened out. These DEGs were significantly enriched in the phagosome and NF-kappa B signaling pathway. Through PPI analysis, *TOP2A*, *TYMS*, *CCNB1*, *RACGAP1*, *FEN1*, *PRC1*, and *UBE2C* were selected as hub genes, which were highly expressed in ATC tissues. TCGA data suggested that the expression levels of *TOP2A*, *TYMS*, *FEN1*, and *PRC1* genes were also upregulated in other histological subtypes of thyroid carcinoma. High expression of *TOP2A*, *TYMS*, *FEN1*, *PRC1*, or *UBE2C* gene significantly decreased disease-free survival of patients with other thyroid carcinomas. In conclusion, the present study identified several hub genes and pathways, which will contribute to elucidating the pathogenesis of ATC and providing therapeutic targets for ATC.

1. Introduction

Thyroid carcinoma is a common endocrine cancer accounting for approximately 1.7% of total cancer diagnoses [1]. The main histologic types of thyroid carcinoma include papillary thyroid carcinoma (PTC), follicular thyroid carcinoma, medullary thyroid carcinoma, and anaplastic thyroid carcinoma (ATC). Approximately 80% of thyroid cancers are PTCs, which are usually curable with a 5-year survival of over 95% [2]. In contrast, ATC constitutes only a small part (1–2%) of all thyroid carcinomas, but it is the most malignant with a median survival of 3–5 months [3, 4]. To date, there is no standard or effective therapy for ATC. Thus, it is very urgent to understand the pathogenesis of ATC, which will contribute to the discovery of the attractive therapeutic targets.

In the past decades, traditional and molecular biological techniques have been used to reveal ATC-related genes and

pathways [5–7]. For instances, Yin et al. found that the downregulated expression of the forkhead box D3 (FOXD3) transcription factor in ATC cells promoted invasiveness and epithelial-to-mesenchymal transition (EMT) and decreased cellular apoptosis. FOXD3 silencing also enhanced p-ERK levels in the ATC cells, suggesting it negatively regulated MAPK/ERK signaling [5]. Zhang et al. observed that S100A4 was highly expressed in ATC tissues. Knockdown of S100A4 significantly decreased proliferation, increased apoptosis, and inhibited the invasive potential of ATC cells [6]. Salerno et al. found that TWIST1 played a pleiotropic role in determining the ATC phenotype. The ectopic expression of TWIST1 induced resistance to apoptosis and increased cellular migration and invasion [7]. Although major efforts to clarify the pathogenesis of ATC are ongoing, the relevant progress is still not obvious. Considering the complexity and heterogeneity of ATC, we adopted microarray technology and bioinformatics methods to systematically explore

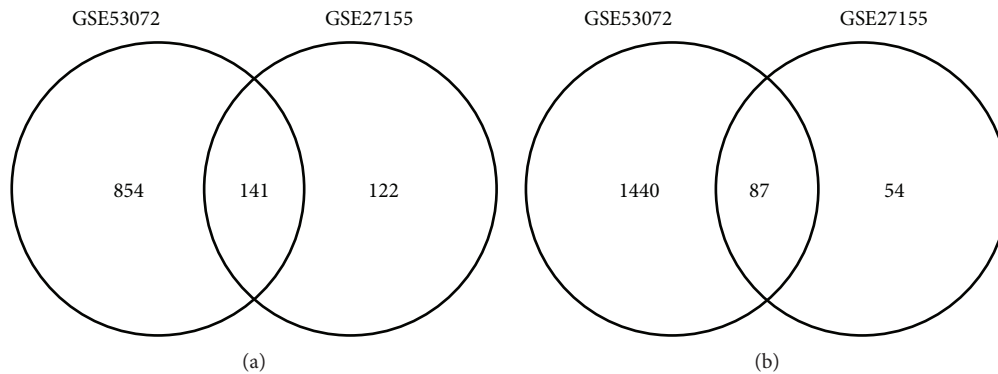


FIGURE 1: Venn diagrams showing the number of differentially expressed genes (DEGs) in ATC tissues compared with normal thyroid tissues ((a) the number of upregulated genes; (b) the number of downregulated genes).

large-cohort gene expression in ATC tissues, which has been demonstrated to be valuable for molecular mechanism investigation [8].

2. Materials and Methods

2.1. Microarray Data. The raw data of gene expression profiles of 9 ATC and 7 normal thyroid tissues were downloaded from Gene Expression Omnibus database (GEO accession numbers: GSE27155 and GSE53072). GSE27155 and GSE53072 datasets were submitted by Giordano et al. and Pita et al., respectively [9–11]. Among these analyzed tissues, 4 ATC and 4 normal thyroid tissues from GSE27155 were detected by Affymetrix Human Genome U133A Array (GPL96 platform). Other tissues from GSE53072 were detected by Affymetrix Human Gene 1.0 ST Array (GPL6244 platform).

The raw data of GSE27155 and GSE53072 were preprocessed using the *affy* and *oligo* packages with the robust multichip averaging (RMA) algorithm, respectively [12–16]. The probeset IDs were converted into the corresponding gene symbols using the annotation information derived from platforms. If multiple probesets correspond to the same gene, the mean expression values of those probesets were obtained.

2.2. Identification of Differentially Expressed Genes (DEGs). Limma R package was applied to identify the DEGs between ATC and normal thyroid tissues [17]. The Benjamini-Hochberg (BH) method was introduced to adjust the raw p values. The adjusted p value < 0.05 and $|\log_2$ fold change (FC)| ≥ 1 were set as the thresholds for identifying DEGs.

2.3. Functional and Pathway Enrichment Analysis of DEGs. In order to systematically explore genes involved in ATC, gene ontology (GO) and pathway enrichment analyses for the common DEGs were performed using the *clusterProfiler* package in R, which was based on the GO and Kyoto Encyclopedia of Genes and Genomes (KEGG) databases [18–20]. The criterion for the significant enrichments was set as p value < 0.05 .

2.4. Construction of the Protein-Protein Interaction (PPI) Network. The PPI network provides a valuable framework for better understanding of the functional organization of the proteome. In this network, nodes and edges represent

proteins and interactions between proteins, respectively. The proteins with high degrees, namely, those highly connected with other proteins, are defined to be located at the network center, which may be regulatory “hubs.” We constructed the PPI network by using STRING database and Cytoscape 3.3 software [21, 22]. The nodes with degree > 1 were reserved in the PPI network. Genes with degree > 25 were considered as hub genes (proteins).

2.5. The Expression Levels of Hub Genes in Other Thyroid Carcinomas. UALCAN (<http://ualcan.path.uab.edu>) is a user-friendly, interactive web resource for analyzing cancer transcriptome data from The Cancer Genome Atlas (TCGA) [23]. In the current study, UALCAN was used to explore the expression levels of hub genes in other thyroid carcinomas. p value < 0.05 was considered statistically significant.

2.6. The Association of Hub Gene Expression with Disease-Free Survival of Patients with Other Thyroid Carcinomas. Gene expression profiling interactive analysis (GEPIA, <http://gepia.cancer-pku.cn/>) is a web-based tool to deliver fast and customizable functionalities based on TCGA and GTEx data [24]. These functionalities included differential expression analysis, profiling plotting, correlation analysis, patient survival analysis, similar gene detection, and dimensionality reduction analysis. In the current study, GEPIA was used to explore the association of hub gene expression with disease-free survival of patients with other thyroid carcinomas. Patients were grouped into high expression group and low expression group according to the median value of hub gene expression. p value < 0.05 was considered statistically significant.

3. Results

3.1. Identification of DEGs. As shown in Figure 1 and Table 1, for GSE27155, a total of 404 DEGs, including 263 upregulated and 141 downregulated genes in ATC, were identified. For GSE53072, a total of 2522 DEGs, including 995 upregulated and 1527 downregulated genes in ATC, were screened out. Further analysis showed that the two independent datasets contained 228 common DEGs, including 141 common upregulated and 87 common downregulated genes in ATC.

TABLE 1: The common differentially expressed genes in GSE27155 and GSE53072 datasets. Note: bold and italic data indicate genes in the phagosome and NF-kappa B signaling pathway, respectively. Bold-italic data indicates the common gene in the phagosome and NF-kappa B signaling pathway.

| | Common differentially expressed genes | | | | | | | | | | | | |
|--------------|---------------------------------------|----------|-----------------|---------------|---------------|---------------|-------------------|--------------|-----------------|--------------|--|--|--|
| | Downregulated genes | | | | | | Upregulated genes | | | | | | |
| MAN1C1 | CA4 | WASF3 | HSD17B4 | CIQA | NCF2 | CLEC7A | RAB31 | COL5A2 | CCNB1 | RAP2C | | | |
| PBX1 | KCNJ16 | CLN5 | MYLIP | CLIC4 | ASPM | RECQL | PMAIP1 | COL6A3 | VCAN | <i>IRAK1</i> | | | |
| Clorf15 | PTRM | RCBTB1 | HSD17B8 | CDC20 | KIF14 | TUBA1A | ADGRE5 | CDC25B | LMNB1 | FLNA | | | |
| MARC2 | TXNL1 | TSHR | MTCHI | VCAM1 | LBR | RACGAP1 | TPM4 | TPX2 | TGFB1 | TAGLN2 | | | |
| MARC1 | CIRBP | SAV1 | KHDRBS2 | GFSM2 | ARID5B | CORO1C | COLGALT1 | UBE2C | SLC36A1 | C3AR1 | | | |
| RAP1GAP | BCAM | DI02 | LMBRD1 | GNAI3 | <i>PLAU</i> | CIT | VASP | CTSA | LHFPL2 | TYMS | | | |
| ECHDC2 | TLE2 | CKB | SLC26A4 | CD53 | ZWINT | ALOX5AP | EMP3 | ADRM1 | CDI4 | WIPF1 | | | |
| PLPP3 | PAX8 | PPP1R13B | EPHB6 | IFI16 | MICAL2 | PNP | PLIN3 | B4GALT5 | TTK | OSMR | | | |
| SELENBP1 | LRP2 | SORD | ATP6V0E2 | FCER1G | MS4A4A | RNASE6 | DDX39A | ITGB2 | RAB32 | KIF4A | | | |
| RGS5 | ACADL | DUOX1 | TMEM243 | FCGR2A | FEN1 | BAZ1A | BST2 | YWHAH | TUBB2A | | | | |
| ALDH9A1 | RAB17 | CRABP1 | EPHX2 | FCGR2B | NNMT | SEC23A | TYROBP | LGALS1 | CLIC1 | | | | |
| RGS16 | SNTA1 | DUOX2 | TG | PTPRC | RHOG | NUSAP1 | AP2S1 | RAC2 | HLA-DPA1 | | | | |
| HHEX | INPP5J | GATM | TJP2 | TRAF5 | LPXN | ANXA2 | RRM2 | GNL3 | TNFRSF21 | | | | |
| <i>PRKCQ</i> | GBX7 | MYO5C | NTRK2 | DTL | MS4A6A | PKM | MTHFD2 | CD86 | THBS2 | | | | |
| NEBL | ACOX2 | DAPK2 | FOXE1 | ENO1 | PPP1R14B | PRC1 | TMSB10 | SMC4 | UPPI | | | | |
| OGDHL | ZBED2 | ABAT | BSPRY | LAPTM5 | Cl Iorf24 | CHSY1 | SLC20A1 | HCLS1 | TMEM176B | | | | |
| ABLIM1 | HGD | SALL1 | CCL21 | YARS | CTSC | CCL13 | ACTR3 | TOPBP1 | EIF4EBP1 | | | | |
| FGFR2 | LIMCH1 | CDH16 | ALDH1A1 | DPYD | TUBA1C | KPNA2 | COL3A1 | TFRC | MCM4 | | | | |
| GLB1L2 | PPARGCIA | ALDH3A2 | CLIC3 | MTMR11 | LYZ | SLC16A3 | PXDN | TLR2 | LY96 | | | | |
| METTL7A | HOPX | DUSP14 | RGN | S100A10 | FOXM1 | EVI2A | MCM6 | H2AFZ | ANXA2P2 | | | | |
| PEBP1 | SORBS2 | HLF | GPRASP1 | S100A11 | TNFRSF1A | TOP2A | RND3 | BASPI | TNC | | | | |
| IFT88 | PDE8B | NAP1L2 | | AIM2 | CD163 | COL1A1 | FAP | SLC1A3 | PLP2 | | | | |

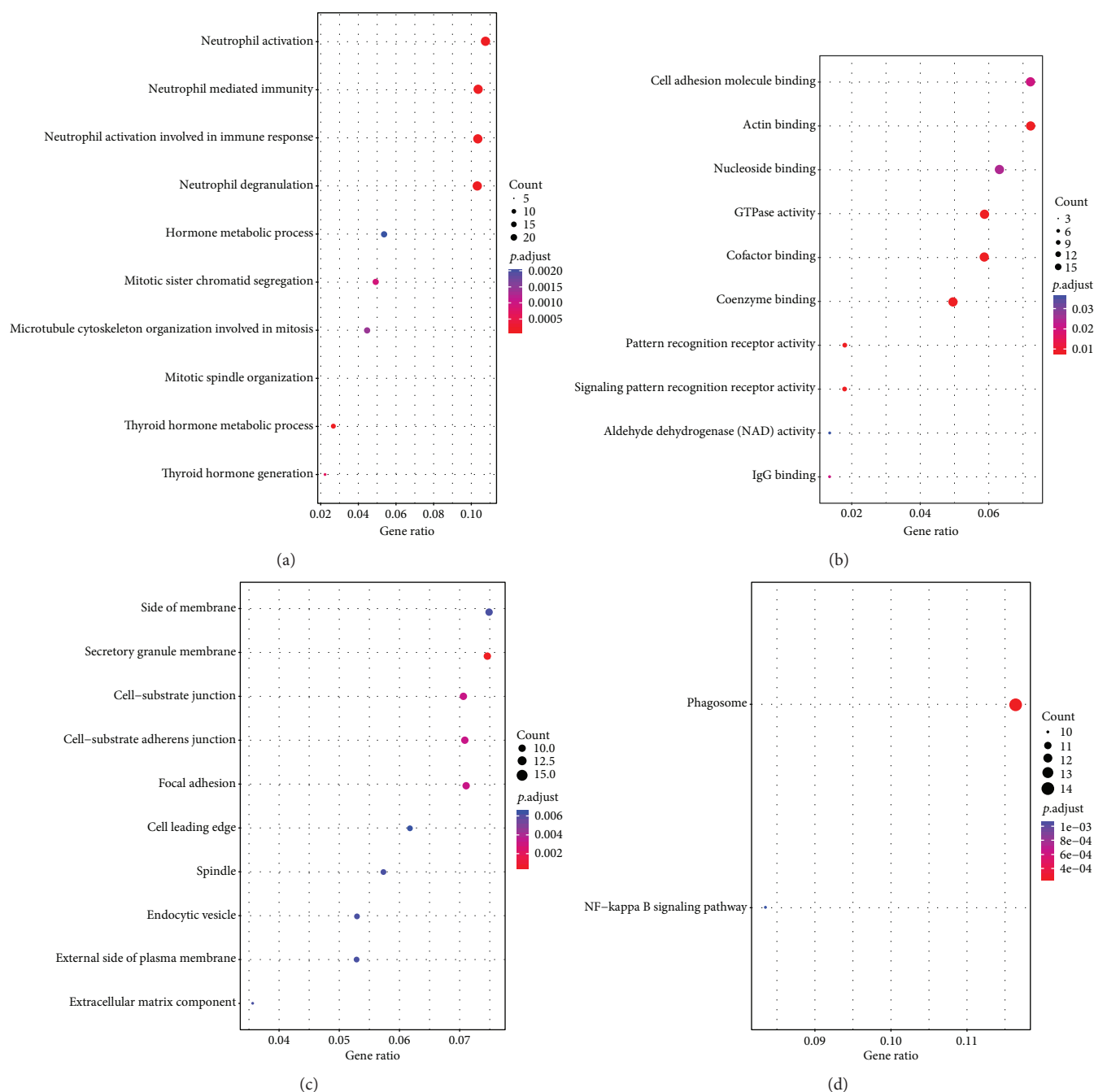
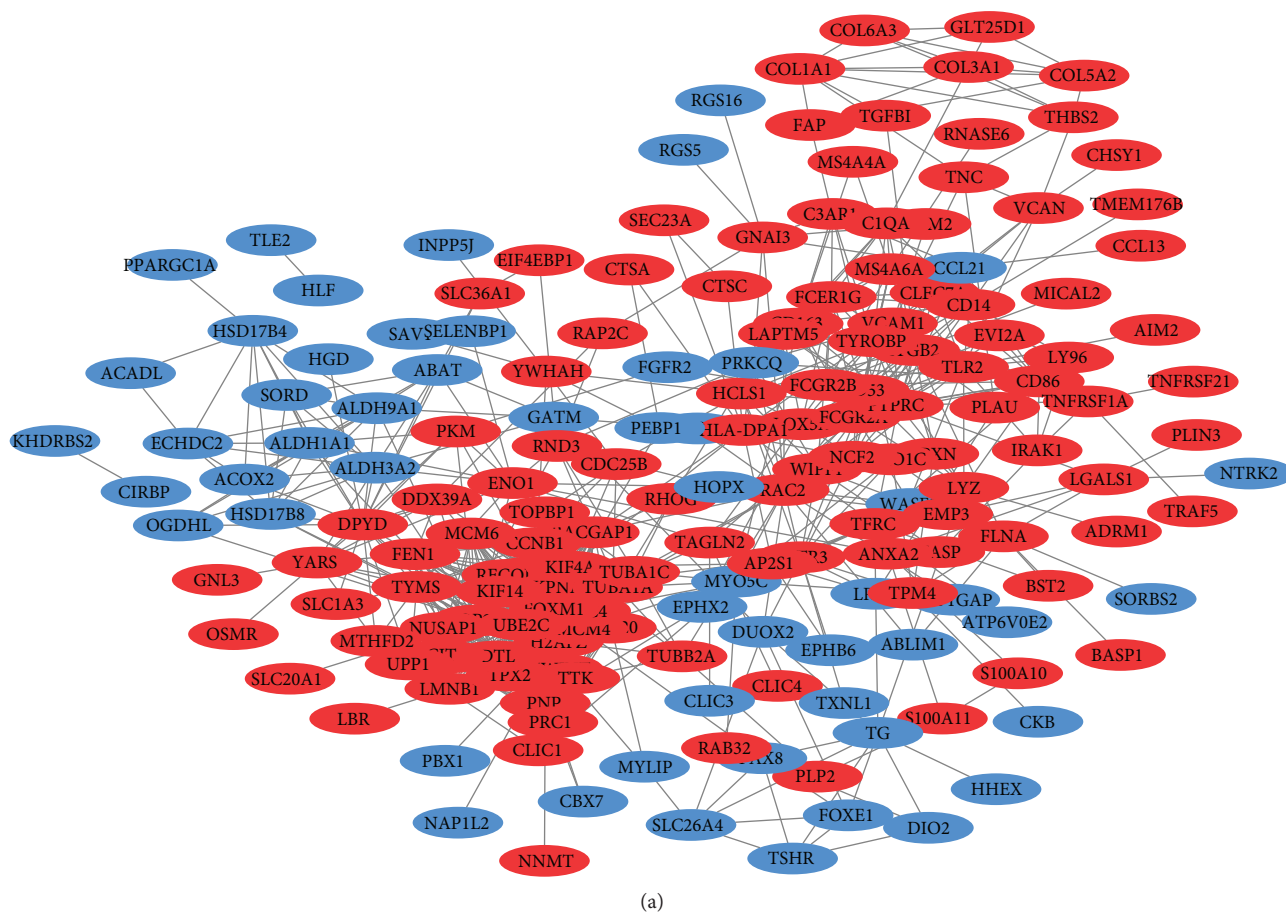


FIGURE 2: The top 10 gene ontology (GO) terms and significantly enriched KEGG pathways ((a) biological processes; (b) molecular functions; (c) cellular components; (d) KEGG pathways).

3.2. Integrated Analysis of the Common DEGs. By GO analysis, we identified 146 significant enrichment terms, which were classified in 3 GO categories, including biological processes (BP, 92), molecular functions (MF, 20), and cellular components (CC, 34). The top 10 GO terms of BP, MF, and CC were shown in Figures 2(a)–2(c). For BP, those common DEGs are significantly enriched in neutrophil activation, neutrophil-mediated immunity, neutrophil activation involved in immune response, neutrophil degranulation, hormone metabolic process, mitotic sister chromatid segregation, microtubule cytoskeleton organization involved in

mitosis, mitotic spindle organization, thyroid hormone metabolic process, thyroid hormone generation, and so on. For MF, those common DEGs are mainly enriched in cell adhesion molecule binding, actin binding, nucleoside binding, GTPase activity, cofactor binding, coenzyme binding, pattern recognition receptor activity, signaling pattern recognition receptor activity, aldehyde dehydrogenase (NAD) activity, and IgG binding. For CC, those common DEGs are significantly enriched in the side of the membrane, secretory granule membrane, cell-substrate junction, cell-substrate adherens junction, focal adhesion, cell leading edge, spindle, and NF-kappa B signaling pathway.



(a)

| Genes | Expression | Degree |
|---------|------------|--------|
| TOP2A | Up | 37 |
| TYMS | Up | 29 |
| CCNB1 | Up | 29 |
| RACGAP1 | Up | 27 |
| FEN1 | Up | 26 |
| PRC1 | Up | 26 |
| UBE2C | Up | 26 |

(b)

FIGURE 3: Protein-protein interaction (PPI) network of differentially expressed genes (DEGs) ((a) PPI network; (b) hub genes).

endocytic vesicle, external side of plasma membrane, extracellular matrix component, and so on. Furthermore, KEGG pathway enrichment analysis showed that these common DEGs were significantly enriched in the phagosome and NF-kappa B signaling pathway (Figure 2(d)).

There were 180 nodes and 737 edges in the PPI network (Figure 3(a)). Thereinto, 7 upregulated genes in ATC, including *TOP2A*, *TYMS*, *CCNB1*, *RACGAP1*, *FEN1*, *PRC1*, and

UBE2C, were selected as the hub genes (Figure 3(b)). *TOP2A* gene had the highest degree (degree = 37) in the network.

UALCAN and GEPIA online tools were used to explore TCGA data. Results suggested that the expression levels of hub genes, *TOP2A*, *TYMS*, *FEN1*, and *PRC1*, were also upregulated in at least one histological subtype of thyroid carcinoma (Figure 4). However, the expression levels of *CCNB1* and *RACGAP1* genes were significantly downregulated in at

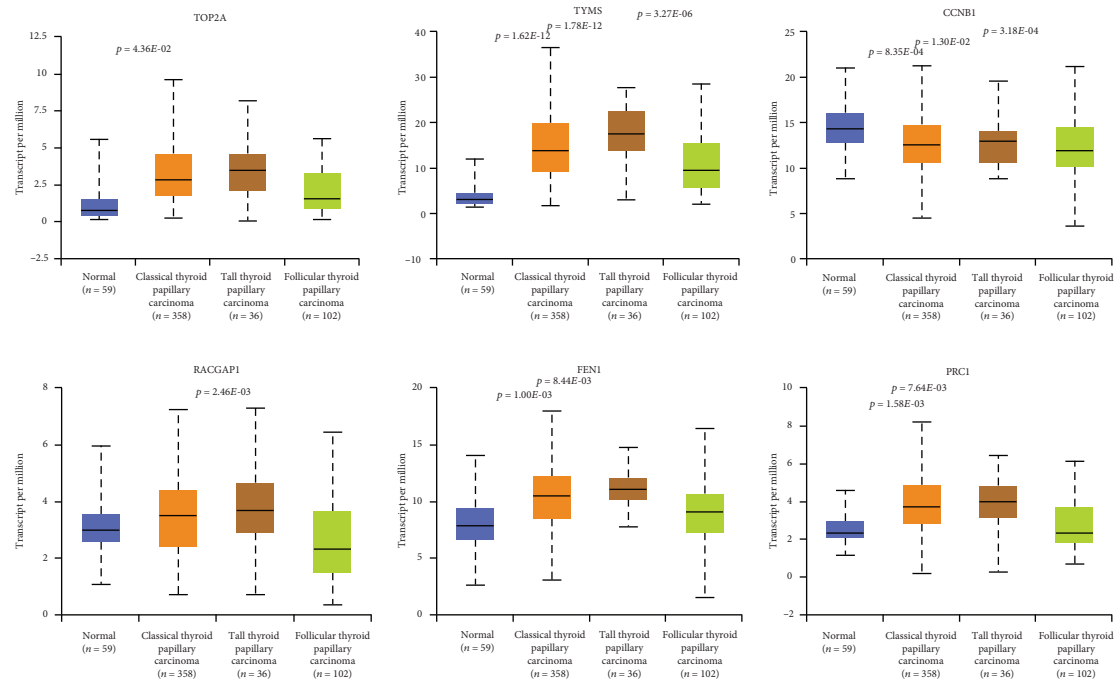


FIGURE 4: The expression levels of hub genes in other thyroid carcinomas.

least one histological subtype of thyroid carcinoma. *UBE2C* gene expression did not significantly change in other thyroid carcinomas (figure not shown). Survival analysis indicated that high expression of *TOP2A*, *TYMS*, *FEN1*, *PRC1*, or *UBE2C* gene significantly decreased disease-free survival of patients with other thyroid carcinomas (Figure 5).

4. Discussion

In the present study, we identified two significant pathways (phagosome and NF-kappa B signaling pathway) and seven hub genes (*TOP2A*, *TYMS*, *CCNB1*, *RACGAP1*, *FEN1*, *PRC1*, and *UBE2C*) related with ATC. In 2017, Huang et al. used GSE33630 data to conduct a similar analysis and considered the Toll-like receptor signaling pathway, extracellular matrix-receptor interaction, and cytokine-cytokine receptor interaction pathway as important pathways implicating ATC. *FOS*, *CXCL10*, *COL5A1*, *COL11A1*, and *CCL28* genes might be used as therapeutic targets for ATC [25]. These findings were different from our findings, which might be attributed to tumor heterogeneity or differences in analytical methods between two studies. Besides the identification of potential hub genes and pathways associated with ACT, we still analyzed the expression levels of these hub genes in other histological subtypes of thyroid carcinoma and found that *UBE2C* gene expression did not significantly change in other thyroid carcinomas, suggesting that *UBE2C* might act as a specific diagnostic biomarker for ACT. Further survival analysis showed that high expression of *TOP2A*, *TYMS*, *FEN1*, *PRC1*, or *UBE2C* gene significantly decreased disease-free survival of patients with other thyroid carcinomas.

Although there was no study directly linking phagosome to ATC, the phagosome participated in the innate and adaptive immune responses [26, 27]. The present study found ten common DEGs involving in the phagosome. Therefore, the role of the phagosome and phagosome-related genes in ATC was worthy of being further explored. NF-kappa B signaling pathway played an important role in cancer initiation and progression [28, 29]. The present analysis of DEGs showed that most genes of the NF-kappa B signaling pathway were upregulated, suggesting that the pathway was also activated in ATC. Furthermore, the NF-kappa B signaling pathway also participated in an anticancer agent (R-roscovitine) activity, inducing apoptosis of ATC cells [30]. These results indicated that novel agents involving the NF-kappa B signaling pathway could be developed to improve ATC treatment.

Previous studies have indicated that seven hub genes identified by the present study play an important role in the occurrence and development of tumors [31–46]. *TOP2A* gene encodes a DNA topoisomerase that controls and alters the topologic states of DNA during transcription. Immunohistochemical analysis showed that *TOP2A* correlated with thyroid tumor histology and it was more frequently expressed in tumors with aggressive clinical behavior [31]. *TYMS* gene encodes thymidylate synthase, which catalyzes the methylation of deoxyuridylylate to deoxythymidylylate. Although the role of *TYMS* in ATC was not reported previously, the enzyme has been of interest as a target for cancer chemotherapeutic agents [32–35]. The protein encoded by *CCNB1* gene is involved in mitosis and necessary for proper control of the G2/M transition phase of the cell cycle. Lin et al. found that dinaciclib, a cyclin-dependent kinase (CDK) inhibitor, could inhibit ATC cell proliferation by

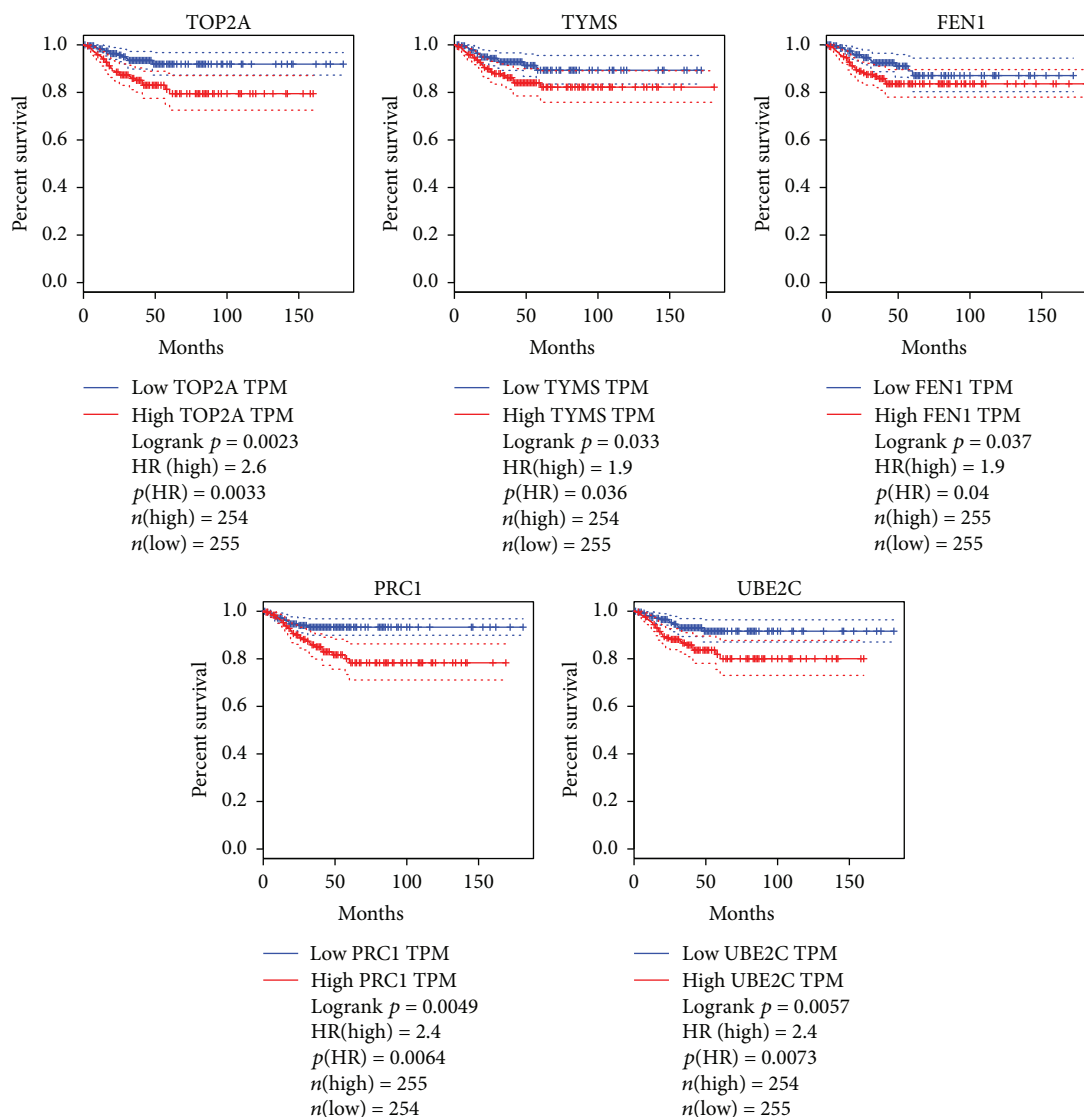


FIGURE 5: The association of hub gene expression with disease-free survival of patients with other thyroid carcinomas.

decreasing CDK1, CCNB1, and Aurora A expression, inducing cell cycle arrest in the G2/M phase and inducing the accumulation of prophase mitotic cells [36]. *RACGAP1* gene encodes a GTPase-activating protein (GAP) that is a component of the centralspindlin complex. This protein played a regulatory role in cytokinesis, cell growth, and differentiation. To date, there is no report linking *RACGAP1* to ATC, but its importance in the development of other cancers has been revealed [37, 38]. The protein encoded by *FEN1* gene removes 5' overhanging flaps in DNA repair and processes the 5' ends of Okazaki fragments in lagging strand DNA synthesis. Previous studies confirmed that *FEN1* not only promoted cancer cell proliferation and progression but also conferred cancer drug resistance [39, 40]. According to these results, we inferred that *FEN1* might also play important roles in development or drug resistance of ATC. *PRC1* gene encodes a protein involved in cytokinesis [41, 42]. The protein is present at high levels during the S and G2/M phases of mitosis, but its levels drop dramatically when the cell exits

mitosis and enters the G1 phase. Recent studies showed that *PRC1* was upregulated in many types of cancer and might serve as a prognostic biomarker of cancer [43–45]. *UBE2C* gene encodes a member of the E2 ubiquitin-conjugating enzyme family. The encoded protein is required for the destruction of mitotic cyclins and for cell cycle progression. Pallante et al. found that *UBE2C* overexpression was involved in thyroid cell proliferation and might act as a diagnostic biomarker for ATC [46].

Taken together, the integrated bioinformatics study presented several hub genes and pathways related to ATC, which would provide new insights into the exploration of pathogenesis and therapeutic targets for ATC.

Data Availability

The microarray data used to support the findings of this study have been deposited in the Gene Expression Omnibus (GEO) repository (accession numbers: GSE27155 and GSE53072).

Conflicts of Interest

The authors declare that they have no competing interests.

Authors' Contributions

Xueren Gao and Jianguo Wang contributed equally to this work.

References

- [1] W. He, B. Qi, Q. Zhou et al., "Key genes and pathways in thyroid cancer based on gene set enrichment analysis," *Oncology Reports*, vol. 30, no. 3, pp. 1391–1397, 2013.
- [2] R. M. Tuttle, D. W. Ball, D. Byrd et al., "Thyroid carcinoma," *Journal of the National Comprehensive Cancer Network*, vol. 8, no. 11, pp. 1228–1274, 2010.
- [3] J. Capdevila, R. Mayor, F. M. Mancuso et al., "Early evolutionary divergence between papillary and anaplastic thyroid cancers," *Annals of Oncology*, vol. 29, no. 6, pp. 1454–1460, 2018.
- [4] E. Molinaro, C. Romei, A. Biagini et al., "Anaplastic thyroid carcinoma: from clinicopathology to genetics and advanced therapies," *Nature Reviews Endocrinology*, vol. 13, no. 11, pp. 644–660, 2017.
- [5] H. Yin, T. Meng, L. Zhou et al., "FOXD3 regulates anaplastic thyroid cancer progression," *Oncotarget*, vol. 8, no. 20, pp. 33644–33651, 2017.
- [6] K. Zhang, M. Yu, F. Hao, A. Dong, and D. Chen, "Knockdown of S100A4 blocks growth and metastasis of anaplastic thyroid cancer cells in vitro and in vivo," *Cancer Biomarkers*, vol. 17, no. 3, pp. 281–291, 2016.
- [7] P. Salerno, G. Garcia-Rostan, S. Piccinin et al., "TWIST1 plays a pleiotropic role in determining the anaplastic thyroid cancer phenotype," *The Journal of Clinical Endocrinology and Metabolism*, vol. 96, no. 5, pp. E772–E781, 2011.
- [8] B. Berger, J. Peng, and M. Singh, "Computational solutions for omics data," *Nature Reviews Genetics*, vol. 14, no. 5, pp. 333–346, 2013.
- [9] T. J. Giordano, R. Kuick, D. G. Thomas et al., "Molecular classification of papillary thyroid carcinoma: distinct BRAF, RAS, and RET/PTC mutation-specific gene expression profiles discovered by DNA microarray analysis," *Oncogene*, vol. 24, no. 44, pp. 6646–6656, 2005.
- [10] T. J. Giordano, A. Y. Au, R. Kuick et al., "Delineation, functional validation, and bioinformatic evaluation of gene expression in thyroid follicular carcinomas with the PAX8-PPARG translocation," *Clinical Cancer Research*, vol. 12, no. 7, pp. 1983–1993, 2006.
- [11] J. M. Pita, I. F. Figueiredo, M. M. Moura, V. Leite, and B. M. Cavaco, "Cell cycle deregulation and TP53 and RAS mutations are major events in poorly differentiated and undifferentiated thyroid carcinomas," *The Journal of Clinical Endocrinology and Metabolism*, vol. 99, no. 3, pp. E497–E507, 2014.
- [12] L. Gautier, L. Cope, B. M. Bolstad, and R. A. Irizarry, "affy-analysis of Affymetrix GeneChip data at the probe level," *Bioinformatics*, vol. 20, no. 3, pp. 307–315, 2004.
- [13] B. S. Carvalho and R. A. Irizarry, "A framework for oligonucleotide microarray preprocessing," *Bioinformatics*, vol. 26, no. 19, pp. 2363–2367, 2010.
- [14] B. M. Bolstad, R. A. Irizarry, M. Astrand, and T. P. Speed, "A comparison of normalization methods for high density oligonucleotide array data based on variance and bias," *Bioinformatics*, vol. 19, no. 2, pp. 185–193, 2003.
- [15] R. A. Irizarry, B. M. Bolstad, F. Collin, L. M. Cope, B. Hobbs, and T. P. Speed, "Summaries of Affymetrix GeneChip probe level data," *Nucleic Acids Research*, vol. 31, no. 4, pp. 15e–115, 2003.
- [16] R. A. Irizarry, B. Hobbs, F. Collin et al., "Exploration, normalization, and summaries of high density oligonucleotide array probe level data," *Biostatistics*, vol. 4, no. 2, pp. 249–264, 2003.
- [17] M. E. Ritchie, B. Phipson, D. Wu et al., "Limma powers differential expression analyses for RNA-sequencing and microarray studies," *Nucleic Acids Research*, vol. 43, no. 7, p. e47, 2015.
- [18] G. Yu, L. G. Wang, Y. Han, and Q. Y. He, "clusterProfiler: an R package for comparing biological themes among gene clusters," *OMICS*, vol. 16, no. 5, pp. 284–287, 2012.
- [19] M. A. Harris, J. Clark, A. Ireland et al., "The Gene Ontology (GO) database and informatics resource," *Nucleic Acids Research*, vol. 32, pp. D258–D261, 2004.
- [20] M. Kanehisa and S. Goto, "KEGG: Kyoto encyclopedia of genes and genomes," *Nucleic Acids Research*, vol. 28, no. 1, pp. 27–30, 2000.
- [21] D. Szklarczyk, J. H. Morris, H. Cook et al., "The STRING database in 2017: quality-controlled protein-protein association networks, made broadly accessible," *Nucleic Acids Research*, vol. 45, no. D1, pp. D362–D368, 2017.
- [22] P. Shannon, A. Markiel, O. Ozier et al., "Cytoscape: a software environment for integrated models of biomolecular interaction networks," *Genome Research*, vol. 13, no. 11, pp. 2498–2504, 2003.
- [23] D. S. Chandrashekar, B. Bashel, S. A. H. Balasubramanya et al., "UALCAN: a portal for facilitating tumor subgroup gene expression and survival analyses," *Neoplasia*, vol. 19, no. 8, pp. 649–658, 2017.
- [24] Z. Tang, C. Li, B. Kang, G. Gao, C. Li, and Z. Zhang, "GEPIA: a web server for cancer and normal gene expression profiling and interactive analyses," *Nucleic Acids Research*, vol. 45, no. W1, pp. W98–W102, 2017.
- [25] Y. Huang, Y. Tao, X. Li et al., "Bioinformatics analysis of key genes and latent pathway interactions based on the anaplastic thyroid carcinoma gene expression profile," *Oncology Letters*, vol. 13, no. 1, pp. 167–176, 2017.
- [26] L. Schnettger and M. G. Gutierrez, "Quantitative spatiotemporal analysis of phagosome maturation in live cells," *Methods in Molecular Biology*, vol. 1519, pp. 169–184, 2017.
- [27] P. Nunes-Hasler, S. Maschalidi, C. Lippens et al., "STIM1 promotes migration, phagosomal maturation and antigen cross-presentation in dendritic cells," *Nature Communications*, vol. 8, no. 1, p. 1852, 2017.
- [28] B. Hoesel and J. A. Schmid, "The complexity of NF- κ B signaling in inflammation and cancer," *Molecular Cancer*, vol. 12, no. 1, p. 86, 2013.
- [29] J. A. DiDonato, F. Mercurio, and M. Karin, "NF- κ B and the link between inflammation and cancer," *Immunological Reviews*, vol. 246, no. 1, pp. 379–400, 2012.
- [30] M. Festa, A. Petrella, S. Alfano, and L. Parente, "R-roscovitine sensitizes anaplastic thyroid carcinoma cells to TRAIL-induced apoptosis via regulation of IKK/NF- κ B pathway," *International Journal of Cancer*, vol. 124, no. 11, pp. 2728–2736, 2009.

- [31] A. Lee, V. A. LiVolsi, and Z. W. Baloch, "Expression of DNA topoisomerase IIalpha in thyroid neoplasia," *Modern Pathology*, vol. 13, no. 4, pp. 396–400, 2000.
- [32] M. Joerger, A. Omlin, T. Cerny, and M. Früh, "The role of pemetrexed in advanced non small-cell lung cancer: special focus on pharmacology and mechanism of action," *Current Drug Targets*, vol. 11, no. 1, pp. 37–47, 2010.
- [33] P. Ceppi, M. Volante, S. Saviozzi et al., "Squamous cell carcinoma of the lung compared with other histotypes shows higher messenger RNA and protein levels for thymidylate synthase," *Cancer*, vol. 107, no. 7, pp. 1589–1596, 2006.
- [34] H. Ozasa, T. Oguri, T. Uemura et al., "Significance of thymidylate synthase for resistance to pemetrexed in lung cancer," *Cancer Science*, vol. 101, no. 1, pp. 161–166, 2010.
- [35] G. Scagliotti, N. Hanna, F. Fossella et al., "The differential efficacy of pemetrexed according to NSCLC histology: a review of two phase III studies," *The Oncologist*, vol. 14, no. 3, pp. 253–263, 2009.
- [36] S. F. Lin, J. D. Lin, C. Hsueh, T. C. Chou, and R. J. Wong, "A cyclin-dependent kinase inhibitor, dinaciclib in preclinical treatment models of thyroid cancer," *PLoS One*, vol. 12, no. 2, article e0172315, 2017.
- [37] C. Wang, W. Wang, Y. Liu, M. Yong, Y. Yang, and H. Zhou, "Rac GTPase activating protein 1 promotes oncogenic progression of epithelial ovarian cancer," *Cancer Science*, vol. 109, no. 1, pp. 84–93, 2018.
- [38] H. Imaoka, Y. Toiyama, S. Saigusa et al., "RacGAP1 expression, increasing tumor malignant potential, as a predictive biomarker for lymph node metastasis and poor prognosis in colorectal cancer," *Carcinogenesis*, vol. 36, no. 3, pp. 346–354, 2015.
- [39] L. He, L. Luo, H. Zhu et al., "FEN1 promotes tumor progression and confers cisplatin resistance in non-small-cell lung cancer," *Molecular Oncology*, vol. 11, no. 9, pp. 1302–1303, 2017.
- [40] K. Zhang, S. Keymeulen, R. Nelson et al., "Overexpression of flap endonuclease 1 correlates with enhanced proliferation and poor prognosis of non-small-cell lung cancer," *American Journal of Pathology*, vol. 188, no. 1, pp. 242–251, 2018.
- [41] C. Mollinari, J. P. Kleman, W. Jiang, G. Schoehn, T. Hunter, and R. L. Margolis, "PRC1 is a microtubule binding and bundling protein essential to maintain the mitotic spindle midzone," *Journal of Cell Biology*, vol. 157, no. 7, pp. 1175–1186, 2002.
- [42] C. Zhu and W. Jiang, "Cell cycle-dependent translocation of PRC1 on the spindle by Kif4 is essential for midzone formation and cytokinesis," *Proceedings of the National Academy of Sciences of the United States of America*, vol. 102, no. 2, pp. 343–348, 2005.
- [43] B. Zhang, X. Shi, G. Xu et al., "Elevated PRC1 in gastric carcinoma exerts oncogenic function and is targeted by piperlongumine in a p53-dependent manner," *Journal of Cellular and Molecular Medicine*, vol. 21, no. 7, pp. 1329–1341, 2017.
- [44] A. Shimo, T. Nishidate, T. Ohta, M. Fukuda, Y. Nakamura, and T. Katagiri, "Elevated expression of protein regulator of cytokinesis 1, involved in the growth of breast cancer cells," *Cancer Science*, vol. 98, no. 2, pp. 174–181, 2007.
- [45] H. W. Luo, Q. B. Chen, Y. P. Wan et al., "Protein regulator of cytokinesis 1 overexpression predicts biochemical recurrence in men with prostate cancer," *Biomedicine & Pharmacotherapy*, vol. 78, pp. 116–120, 2016.
- [46] P. Pallante, M. T. Berlingieri, G. Troncone et al., "UbcH10 overexpression may represent a marker of anaplastic thyroid carcinomas," *British Journal of Cancer*, vol. 93, no. 4, pp. 464–471, 2005.